Reply to community comment

Thank you for your constructive comments, which are very helpful to improve the paper and clarify our points. Our point-by-point reply follows with the original comments quoted in `Courier` font.

1. `If the authors explain the behavior of predicted radiative cooling shown on their Fig. 9. In particular, why is it so small after the initial surge?`

Following the fog formation, a substantial increase in the fog-top entrainment weakens the liquid water gradient at the fog top, subsequently diminishing the radiative cooling (Fig. S1). Figure S2 depicts the lagged correlations between the entrainment at the fog top and the LWC within the fog layer and at the fog top. The correlations peak with a lag of 5 and 10 hours for the layer-averaged and fog-top LWC, respectively. This indicates that it takes several hours for the entrainment to weaken the radiative cooling Another reason is the rapid growth of the fog layer depth during the initial phase(Fig. S3). We added the related descriptions (lines 389-395).

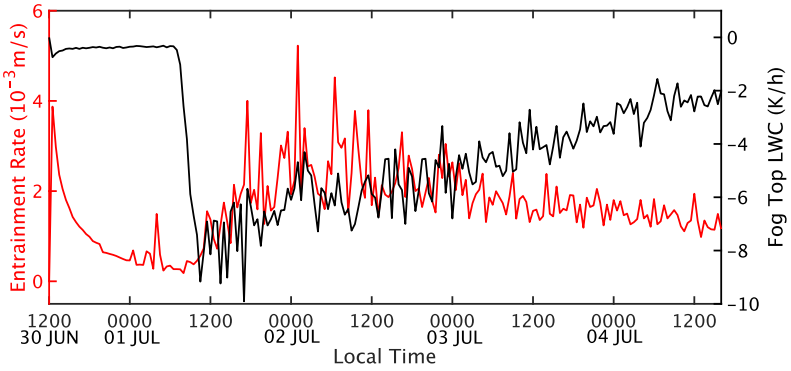

FIG. S1 Time series of entrainment rate (red line) and LWC rate at fog top (black line) for the constant solar radiation simulation. The fog top is defined as the height where the maximum LWC rate occurs.

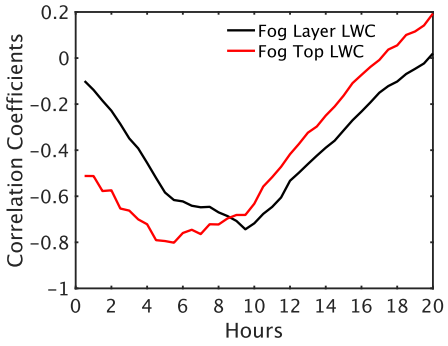

FIG. S2 Lagged correlation coefficients of the fog-top entrainment with LWC for integral boundary layer (black line) and at fog top (red line). The fog top is defined as the height where the maximum LWC rate occurs.

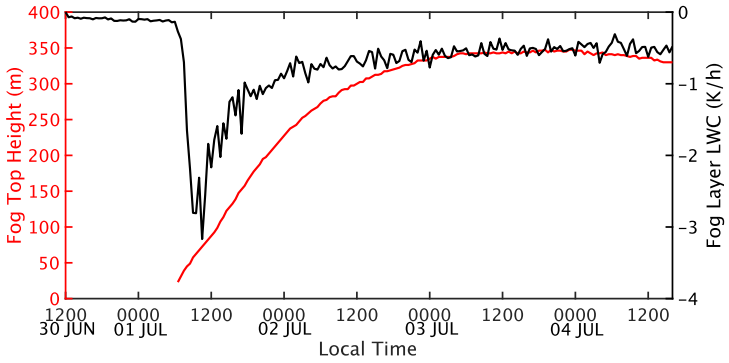

FIG. S3 Time series of LWC for the integral fog layer (black line in K h^{-1}) and fog top height (red line in m) for the constant solar radiation simulation.

2. Also, this ir cooling amount is substantially less than in stratocumulus under clear sky conditions, assuming that this cooling acts similarly for advection fog and for stratocumulus (e.g., see Gerber et al.: 14th AMS Conf. on Atm. Radiation, 7-11 July, 2014, Boston, MA., paper 9.3.).

Current Fig. 10 shows the heat budget for the fog layer, which differs from the heat budget profiles in previous studies (Curry and Herman 1985; Fu and Liou 1992; Gerber et al. 2014). We also examined the time-series maximum in LWC profiles (Fig. S4), which fluctuates around 8 K h^{-1} after fog formation and then steadily decreases. The fog-top LWC is somewhat less than the counterpart for typical stratocumulus clouds (Gerber et al. 2014). This may be attributed to the difference in free atmospheric humidity between fog and stratocumulus scenes. In the case of stratocumulus clouds, the corresponding descending motion results in drier air compared to the free atmosphere above fog. We added the related descriptions (lines 395-401).

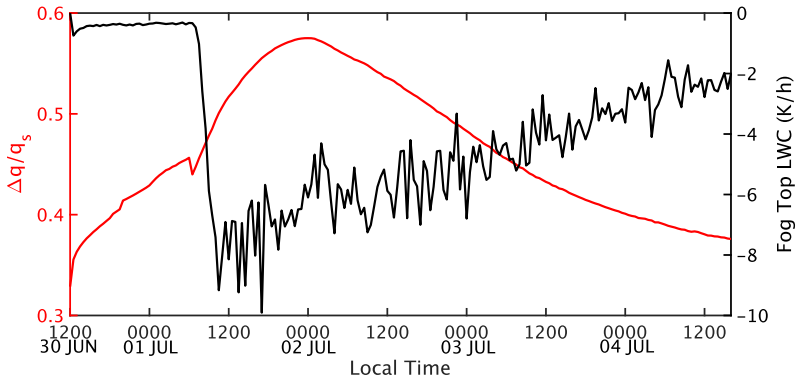

FIG. S4 Time series of humidity stratification (red line) and LWC rate at fog top (black line) for the constant solar radiation simulation. The humidity stratification is the differences in averaged specific humidity between boundary layer and 1–2 km that is normalized by the surface saturation specific humidity. The fog top is defined as the height where the maximum LWC rate occurs.

3. Further, can you comment on the grid spacing used in your model if it is sufficient to deal with the details of the usually very

narrow fog-top interface that may need sub-grid parameterization.

We increased the vertical resolution to 1 m below 50 m and 5 m above 50 m. The simulation produces smoother variation in fog top height and stronger liquid water content at the fog top compared with the original simulation. The dissipation time of sea fog is delayed by 12 hours. However, the main conclusions remain unchanged. We substituted the analyses and results in this paper with simulations at a higher vertical resolution (lines 148-150, Figs. 6-14).

Reply to Review #1

Thank you for your constructive comments, which are very helpful to improve the paper and clarify our points. Our point-by-point reply follows with the original comments quoted in `Courier` font.

1. `Title: Solar radiation is included in all of the analysis, so not sure why the authors have "longwave" in the title?`

   We removed "longwave" in the title.

2. `Figure 6c suggests that there is a lot of cloud water in the fog. Especially towards the end the cloud water content is constant at ~1 g/kg throughout the layer. I assume that at this high value, there is got to be some cloud water to rainwater conversion. Now if the rain is leaving the fog and falling into the sea surface, it will thin the fog layer and also affect the budget terms. Normally the surface rain flux is a heating and drying term in boundary layer budgets, see Caldwell and Bretherton (2005 JAS). Can you please expand on this a bit more? The cloud droplet number concentration is set constant in the simulations, but there is no mention of rain, so it is hard to tell what might cause this. Lack of rain might be the reason that the fog is persisting over a long time. I assume there are no aerosols in the model.`

We calculated the sedimentation (F_p) term from moisture budget. The precipitation term is calculated using the total water budget equation (Caldwell and Bretherton, 2005),

$$\frac{\partial \overline{q_t}}{\partial t} = -\frac{\partial \overline{w'q_t'}}{\partial z} + F_p \tag{1}$$

where q_t is total water mixing ratio. The terms on the *RHS* describe the q_t change from turbulent mixing effect and droplet sedimentation. The sedimentation term is provided as a source/sink term for q_t budget. The advection and molecular diffusion terms are omitted as their magnitudes are much smaller than other terms in the equation. Total water (q_t) can be divided into water vapor (q_v) and liquid water (q_l), their budget equations are:

$$\frac{\partial \overline{q_v}}{\partial t} = -\frac{\partial \overline{w'q_v'}}{\partial z} + \frac{E}{\overline{\rho}} \tag{2}$$

$$\frac{\partial \overline{q_l}}{\partial t} = -\frac{\partial \overline{w'q_l'}}{\partial z} - \frac{E}{\overline{\rho}} + F_p \tag{3}$$

The $\overline{w'q_v'}$and $\overline{w'q_l'}$ are turbulent water vapor flux and turbulent liquid water flux, respectively. The sedimentation effect on heat budget is calculated using the following quation,

$$\frac{\partial \bar{\theta}}{\partial t} = -\frac{\partial \overline{w'\theta'}}{\partial z} - \frac{L_v E}{\bar{\rho} C_p} - \frac{1}{\bar{\rho} C_p}\frac{\partial \bar{Q}}{\partial z} - \frac{L_v F_p}{C_p}, \quad (4)$$

where the last term is the sedimentation term.

The precipitation primarily contributes to the liquid water budget. The liquid water generation is most pronounced at the top of the fog, leading to a peak in liquid water content at the fog top. Large cloud water content converses into rainwater and descends, resulting in a secondary peak of liquid water near the surface at about 20 m (Fig. S5a). However, within the boundary layer and at surface, sedimentation has a drying effect. The impact of sedimentation for the heat budget is relatively small compared to turbulent mixing and LWC, both at surface and within the boundary layer (Fig. S5b). We added the related descriptions (lines 335-336, and 359-362).

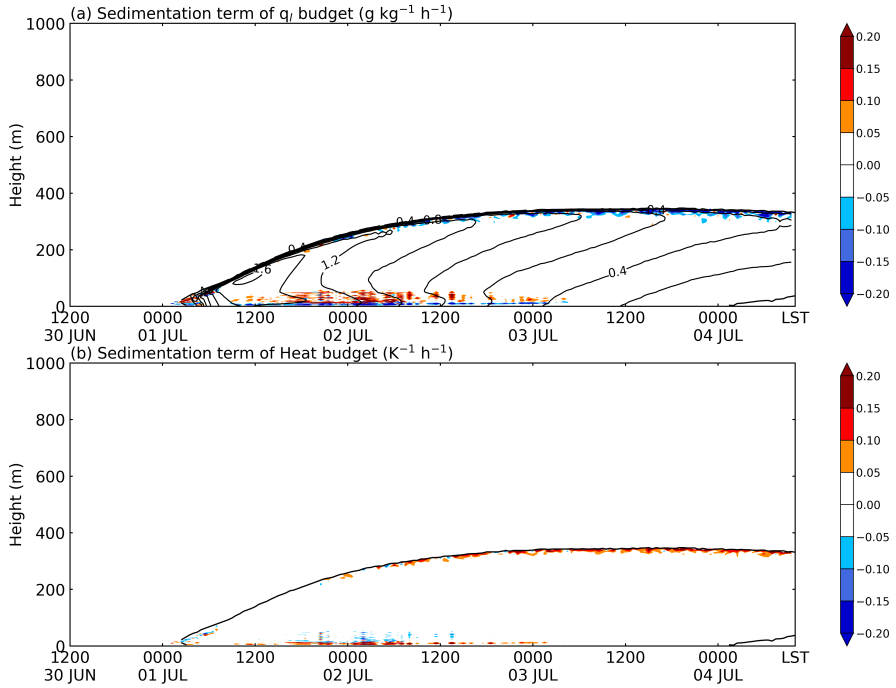

FIG. S5 Horizontal mean sedimentation term for (a) liquid water (g kg^{-1} h^{-1}) and (b) heat (K h^{-1}) budget. Contours in (a) are liquid water mixing ratio (g kg^{-1}) and black lines in (b) indicates fog top and bottom.

We also calculated the sedimentation term for moisture and heat budget using turbulent liquid water flux (Caldwell and Bretherton, 2005):

$$\frac{\partial \overline{q_t}}{\partial t} = -\frac{\partial \overline{w'q_t'}}{\partial z} - \frac{\partial \overline{w'q_l'}}{\partial z} \quad (5)$$

$$\frac{\partial \bar{\theta}}{\partial t} = -\frac{\partial \overline{w'\theta'}}{\partial z} - \frac{L_v E}{\bar{\rho} C_p} - \frac{1}{\bar{\rho} C_p}\frac{\partial \bar{Q}}{\partial z} - \frac{1}{\bar{\rho} C_p}\frac{\partial \overline{w'q_l'}}{\partial z} \quad (6)$$

The results still show that the sedimentation term has a relatively small impact on the moisture and heat budget (Fig. S6).

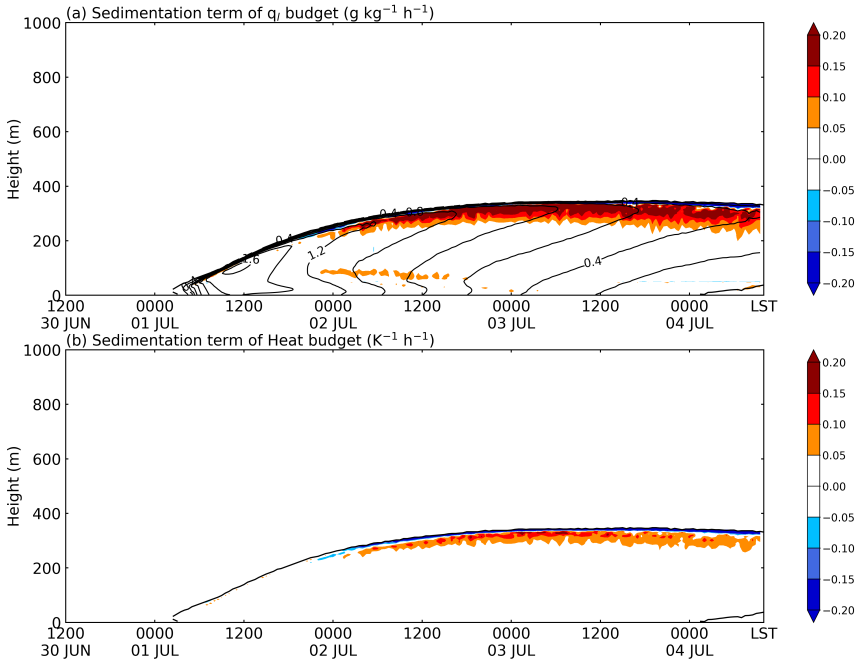

FIG. S6 The same as Fig. S5 but the sedimentation rate is calculated using turbulent liquid water flux.

3. Section 2.2: please mention the vertical and horizontal resolution of the LES model.

We added resolution information in lines 148-150.

4. Line 151-152: you mean "respectively"?

Revised (line 158).

5. Line 169-170: How were the fog events tracked, was there a trajectory model used for this analysis?

We tracked the fog observations by integrating ERA5 10-m winds and validated the obtained trajectory in Fig. 5 using the HYSPLIT (Draxler and Rolph, 2010). The trajectory in Fig. 4 is roughly consistent with the trajectory based on HYSPLIT (red line in Fig. S7). We added the related descriptions (lines 176, and 260-261).

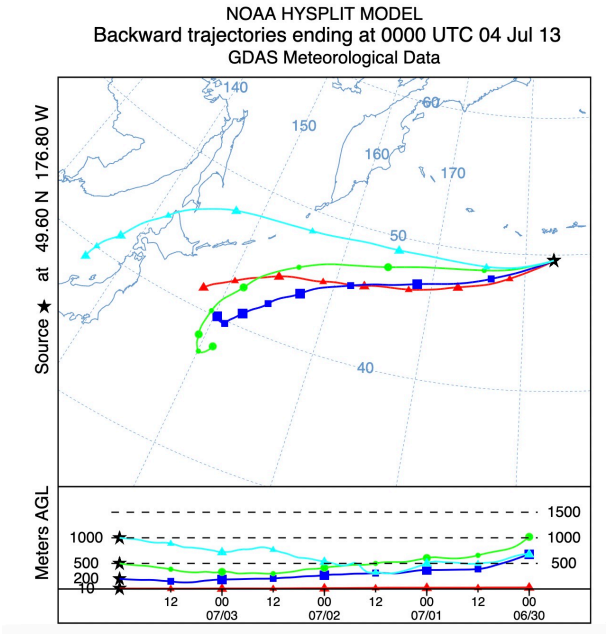

FIG. S7 4-day backward trajectory from the ssH fog observation at 49.6°N 183.2°E reported at 1000 LST (0000 UTC) on 04 July. The tracked height for air parcels includes 10 m (red line), 200 m (blue line), 500 m (green line) and 1000 m (light blue line).

6. Figure 1: Please show the scale of the wind barb and mention the contour levels. I understand that you have mentioned two SST contours in the legend shown in thick lines, but it will be good to show them in the figure.

   We added wind barb scale and contour levels onto Fig. 1.

7. Figure 4: A lot of work has gone into this figure. I think snapshots of visible satellite imagery will be hugely beneficial to the readers.

   We added satellite images and theirrelated descriptions (Fig. 3, lines 221-223, and 230).

8. Section 4.2 heading: "Heat and Moisture Budgets"

   Revised (line 346).

9. Figure 10b and Figure 12 are fascinating. Compared to those in the constant solar radiation simulations, the fog layer bottom and top undulate a lot during the diurnal cycle simulations. Can you please elaborate causes of this? Thank you.

During the night, the strengthening of the fog-top LWC enhances thermal turbulence and the entrainment (Fig. S8), thereby bringing in more air into the fog layer and causing an increase in the fog top height. Conversely, during the day, the weakened the fog-top LWC reduces entrainment (Fig. S8), leading to a decrease in the fog top height. With the continued drying effect of entrainment, the liquid water content in the fog layer decreases. The cooling effect of the LWC gradually becomes weaker than the drying effect of entrainment, ultimately causing the transition into stratus. The cloud

base height rapidly rises and decreases during night due to the absence of the solar radiation. We added the related descriptions (lines 455-460).

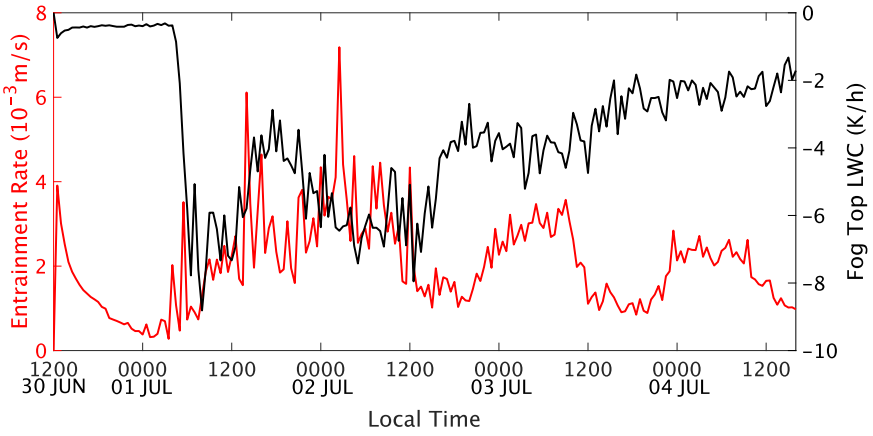

FIG. S8 Time series of entrainment rate (red line) and LWC (black line) at the fog top for the simulation with diurnal cycle radiation.

Reply to Review #2

Thank you for your constructive comments, which are very helpful to improve the paper and clarify our points. Our point-by-point reply follows with the original comments quoted in `Courier` font.

Minor comments

`1. 2.2. How are surface fluxes prescribed / computed?`

The model supports different methodologies for specifying the subgrid fluxes at the lower boundary. They can be prescribed, calculated based on prescribed gradients, or prescribed surface properties. For the latter two, similarity functions are chosen to relate the fluxes at the surface to the grid-scale gradients there (Stevens et al., 2010). The similarity functions used by the model are as follows,

$$\Phi_h = \frac{\kappa z}{\theta_*}\frac{\partial \bar{\theta}}{\partial z} = \begin{cases} \Pr(1 + a_h\zeta) & \zeta > 0 \\ \Pr(1 - b_h\zeta)^{-1/2} & \zeta \le 0 \end{cases}$$

$$\Phi_m = \frac{\kappa z}{u_*}\frac{\partial \bar{u}}{\partial z} = \begin{cases} \Pr(1 + a_m\zeta) & \zeta > 0 \\ \Pr(1 - b_m\zeta)^{-1/2} & \zeta \le 0 \end{cases}$$

where $\zeta = \frac{a}{\lambda}, \lambda = \frac{\Theta_0}{gk}\left(\frac{{u_*}^2}{\theta_*}\right)$ is the Monin-Obukov length scale. The similarity constants are $\Pr = 0.74, \kappa = 0.35, a_h = 7.8, a_m = 4.8, b_h = 12, b_m = 19.3$. In this article, we set specific surface properties to be over the ocean and prescribe surface temperature and specific humidity. We added the related descriptions (lines 138-140).

`2. Fig. 1. Is there any difference, in terms of detection, between fog and advection fog? The caption says fog but the section equates it to advection fog. Only in L219 there is a mention of a combined criterion for advection fog.`

We got advection fog by tracing back each fog observation. Compared to the advection fog frequency, the frequency of all fog is higher, especially over the Sea of Okhotsk (Fig. S9). However, the overall patterns are quite similar between the two. The observational discussions in this article are all related to advection fog, as well as the phenomena of ssH and ssC within advection fog. We revised the caption in Figs. 1 and 2 and clarified our choice of advection fog in lines 176-180.

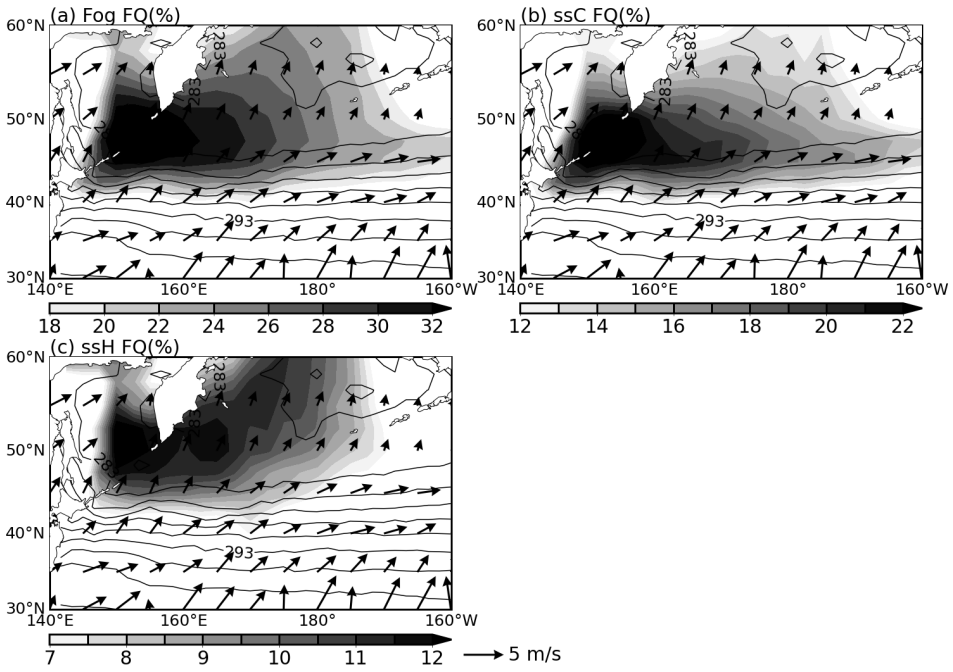

FIG. S9 Climatological SST (contours with 2-K intervals), surface winds (vectors, m s^{-1}), and frequencies (shading, %) of (a) fog, fog with (b) ssC and (c) ssH during June-July-August for 1998-2018. The SST and winds are based on ERA5, and the fog frequencies are obtained from ICOADS.

3. L240 Here it seems like there is enough information to make a timeseries of the observational SAT-SST. Would that be possible to add in order to compare the model results?

Very nice suggestion, Thanks. We added the time series of observational SAT-SST using ICOADS (Fig. 5) and the related descriptions (lines 232-236, 307-309, and 463-464).

4. More details about the LES configuration are needed. It references Yang et al. (2021) but the manuscript should be self contained. How are the initial profiles determined, is there any modification from the ERA5 vertical profiles? Is the initial profile cloudy or clear? Does the referenced paper work with the same case? I'm understanding that SST(t) is prescribed, are winds nudged?

We mentioned thesimulation setups in lines 264-280.

5. L244 Any reason to choose that value of divergence? I assume it can definitely affect the results by modifying the BL top height and LW cooling

The divergence is an averaged divergence along the trajectory in Fig. 4. We chose the realistic synoptic condition instead of the climatological divergence in Yang et al. (2021) to reproduce the advection fog with ssH (lines 267-270).

6. L255 Is this quick growth realistic when compared to observations?

Cloud–Aerosol Lidar and Infrared Pathfinder Satellite Observations (CALIPSO) passed through the fog area and observed cloud-top heights of about 300 m and 400 m on 0000 LST 02 July and 0100 LST 03 July, respectively (Fig. S10). The simulated grouth of fog thickness is very close to the CALIPSO observations. We mentioned this comparision in lines 290-293. In addition, we found the fog top reach its equilibrium after ~48 hours in our current simulation with higher vertical resolution, comparing 24 hours in our previous simulation.

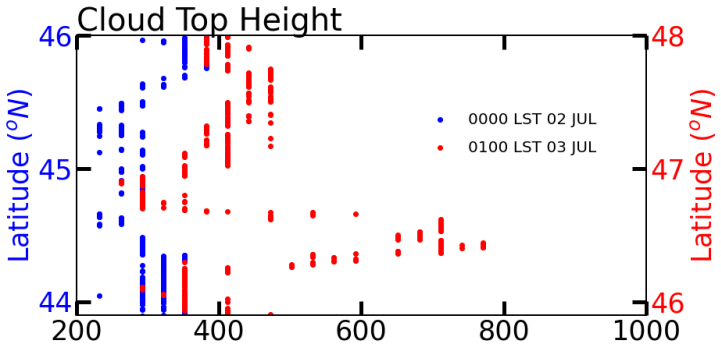

FIG. S10 Cloud-top height observed by CALIPSO data at 0000 LST 02 July (blue dots) and 0100 LST 03 July (red dots).

7. L256 Does the inversion strength grow due to BL cooling or to changes above the BL?

The fog layer cooling strengthens the inversion. The variation in free-atmospheric potential temperature is rather small (Fig. 7a, line 294).

8. L272 The four phases could be shown in the figures: Fig 5,7,10 as different shaded areas, and in Fig 6 as the labels (instead of times)

Revised (Figs. 6, 7, 8, and 11).

9. L278 Would a shorter averaging time window give sharper vertical profiles?

The vertical profiles change slightly between the soundings 2-hour averaged and at specific time (Fig. S11). We used the profiles at specific time in Fig. 7.

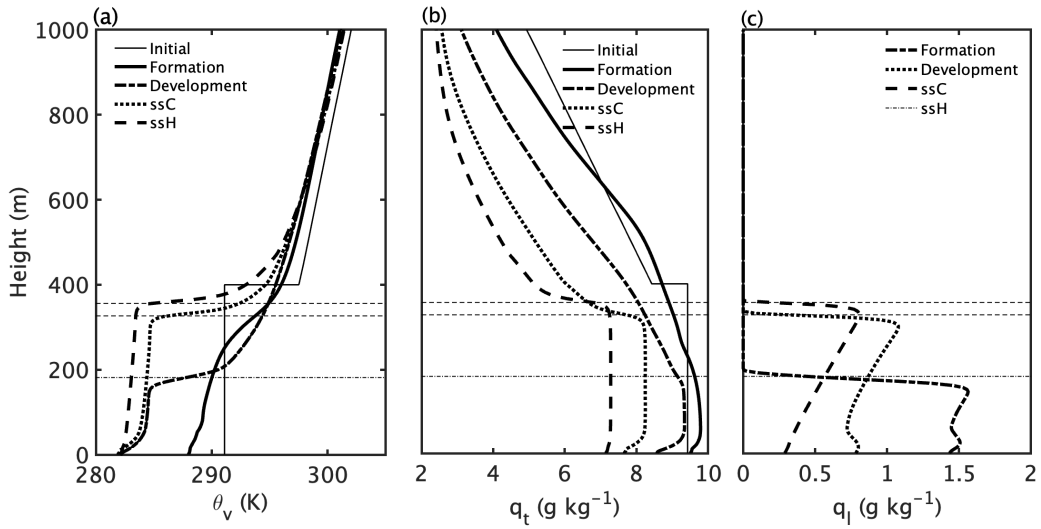

FIG. S11. Horizontal mean soundings at the specific times.

10. L309 Do you mean that LW cooling is directly related to a colder SST?

We revised this description (lines 349-351).

11. L336 Here I got a bit confused, so 'SH' is just the sensible heat flux and 'Ent' is w′ θ′ t(zi)? By integral do you mean across the BL?

Correct. 'SH' represents surface sensible heat flux and 'entrainment' is turbulence heat flux at fog top ($\overline{w'\theta'}_{z_i}$). We quantify the heat budget for the fog layer by integrating heat budget. We clarified this point in lines 379-381.

12. Fig. 10. Why include the diurnal case here? It has not been done for the previous figures

The diurnal case panel in Fig. 10 was moved to current Fig. 14.

13. L371 I don't follow this argument, is it related to LW cooling attenuation for having more water content above?

The TKE budgets have a bit differences in our current simulation with higher vertical resolution. We revised this description (lines 427-430).

14. L377 I'm not familiar with the interpretation of the thermal turbulence interface, what does it add to the discussion?

The thermal turbulence interface helps to separate the fog layer into the zones dominated by LWC and surface cooling. We also added the related descriptions of the method (lines 437-443).

15. 5. I wonder if this section can bring more questions, such as the effect of dynamical changes on the evolution of the fog layer. In the end, for fog lifetime, does it matter if it's modeled with constant solar irradiance? When the sun goes down, how long

does it take the layer to react? Does the stronger solar irradiance accelerate BL processes? How do these results compare to the observations?

Focusing on the simulation with diurnal variation, the maximum fog layer height is similar to the constant solar radiation simulation, as well as the daily averaged sea–air thermal and moist differences (Figs. 6 and 13). We calculated the heat budget for the integral fog layer for the simulation with diurnal solar radiation (Fig. S12). After fog formation, the LWC effect rapidly exceeds surface cooling 4 hours after fog formation and dominates the boundary layer cooling. The LWC at fog top has a clearer diurnal variation which dominates the SAT-SST (Fig. S13). About 3-5 hours before sunset, LWC at fog top reaches its weakest during a day, and then start to strengthen. The enhancement of LWC occurs approximately 3 hours earlier than the decline in air-sea temperature difference, ultimately causing the air temperature falls below the SST in the early hours of 03 July, consistent with the observed time of ssH fog occurrence (Fig. S13 and Fig. 5). We added the related descriptions (lines 466-471).

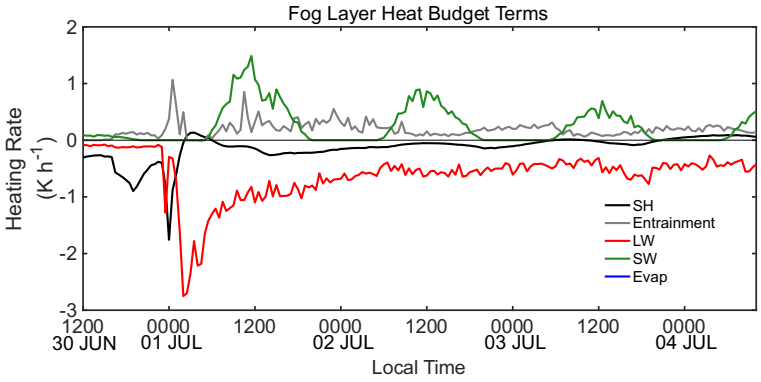

FIG. S12. Time series of horizontal mean heat budget terms (K h^{-1}) of the integral boundary layer for the simulation with diurnal solar radiation.

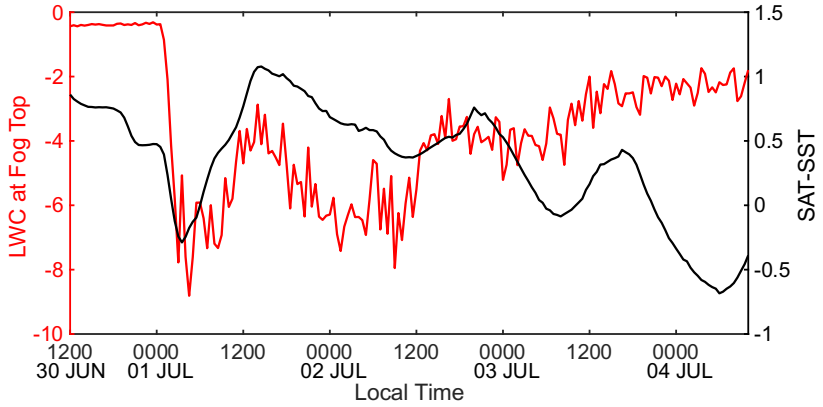

FIG. S13. Time series of horizontal mean LWC at fog top (red line) and SAT-SST (black line) for the simulation with diurnal solar radiation.

The insolation in the constant solar radiation experiment is 518 W m^{-2} at 2000 m (solar elevation angle is 63°), which is the diurnally averaged value from 30 June to 4 July 2013. We conducted a simulation with increased solar irradiance with 66° of solar elevation angle of. Sea fog

dissipates 8 hours earlier than that in the standard solar radiation experiment and observations (Figs. S14, 5 and 6). Two hours before sea fog dissipation, there is the ssH fog occurrence, which appeares two hours earlier than in the standard solar irradiance experiment and in observations (Figs. S14, 5 and 6). Nevertheless, there are little changes in the evolution of the fog top height and the thermal/turbulent structure of the boundary layer during sea fog. We added descriptions in lines 477-482.

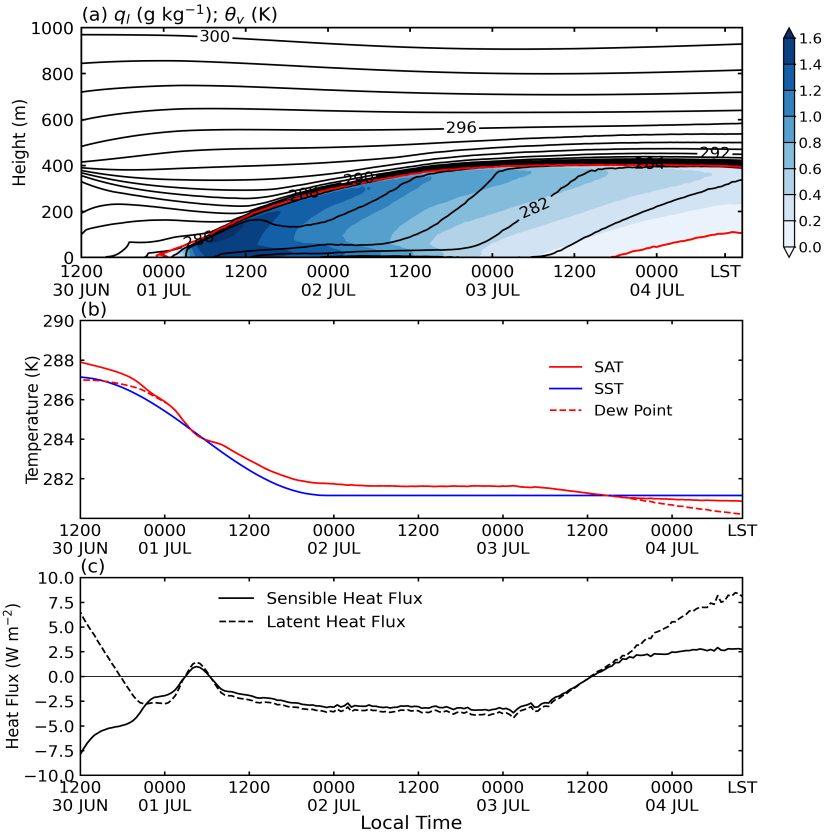

FIG. S14. Time series of horizontal mean LWC at fog top (red line) and SAT-SST (black line) for the simulation with diurnal solar radiation.

16. 6. In this section, many quantitative results for the constant solar irradiance are summarized, but not for the observational nor the varying solar case. It would be better to discuss the three if possible. How does this study relate to other modeling works other than Yang et al. (2021)? Is there anything novel in that regard to report? It would be good to not only include discussion with other works here but also in section 5, in order to support the description and explanations given. How do you propose that the modeling gap in larger models could benefit from this knowledge, in a practical sense?

We added more discussions in lines 507, 509, 522-559.

17. L453 I'm not sure where that comparison is

We revised the sentence in lines 560-565.

Writing comments / suggestions

1. In general, the manuscript is well written. Out of personal style, I'd recommend checking thoroughly the use of the article "the" over the document

   We revised the use of "the" throughout the manuscript.

2. L21 maybe it's better to say the difference, not sure if SAT-SST will be understood

   Revised (lines 21-22).

3. L26 "arrives at"

   Revised (line 26).

4. L28 "well simulates" means that it matches the observations, right?

   Revised (line 29).

5. (1) what is E?

   E in equation (1) is the amount of water vapor produced by liquid phase transition. Revised (line 159).

6. L52 It is unusual to start a sentence with a symbol, though this could be a matter of style, I'd suggest to use commas an evaluate the use of more "the" in this paragraph

   Revised (lines 49-52).

7. L132 Turbulent fluxes are not part of the prognostic variables, right?

   Turbulent fluxes are parameterized. Revised (lines 131-132).

8. L160 "moisture variations"

   Revised (line 166).

9. (3) Shouldn't the buoyant term only have u3?

   Revised (equation 3).

10. L170 "wind fields from ERA5"

Revised (line 176).

11. L173 "(ssC, when SAT-SST>0)"

Revised (line 179).

12. L190 "are positive" instead of "exceed 0°C"

Revised (line 196).

13. L306 "budget terms"

Revised (line 347).

14. Fig 8 "heat and moisture"

Revised (Fig. 9).

15. L330 "weakens and the turbulent mixing cooling dominates"

Revised (lines 372-373).

16. L432 "analyzed in the detail"

Revised (line 511).

17. L439 "column"

Revised (line 518).

Reference

Caldwell, P., Bretherton, C. S., & Wood, R. (2005). Mixed-layer budget analysis of the diurnal cycle of entrainment in southeast Pacific stratocumulus. *Journal of the Atmospheric Sciences*, 62(10), 3775-3791.

Curry, J.A., & Herman, G. F., (1985). Infrared radiative properties of summertime Arctic stratus clouds. *Journal of Climate Apply Meteoroligy*, 24, 525-538.

Draxler, R. R., & Rolph, G. D. (2010). HYSPLIT (HYbrid Single-Particle Lagrangian Integrated Trajectory) model access via NOAA ARL READY website (http://ready. arl. noaa. gov/HYSPLIT. php), NOAA Air Resources Laboratory. *Silver Spring*, MD, 25(1).

Fu, Q., & Liou, K. N. (1992). On the correlated k-distribution method for radiative transfer in nonhomogeneous atmospheres. *Journal of Atmospheric Sciences*, 49(22), 2139-2156.

Gerber, H., Malinowski, S., Bucholtz, A. & Thorsen, T. (2014). Radiative Cooling of Stratocumulus. Extended Abstract. 14 Atmospheric Radiation Conference, American Meteorology Society, Boston, MA, 7-11 July, paper 9.3.

Stevens, B. (2010). Introduction to UCLA-LES: Version 3.2. 1. MPI Doc., 20 pp.